DEVELOPMENTS IN NDT OF FRICTION STIR WELDING USING EDDY CURRENTS

Telmo G. SANTOS[1,2], Pedro VILAÇA[1], Luís ROSADO[3], Moisés PIEDADE[3], Pedro M. RAMOS[4]

[1]IDMEC, Instituto de Engenharia Mecânica, Av. Rovisco Pais, 1, 1049-001 Lisbon, Portugal
[2]Faculdade de Ciências e Tecnologia, FCT, Universidade Nova de Lisboa, 2829-516 Caparica, Portugal
[3]DEEC, Instituto Superior Técnico, Av. Rovisco Pais, 1049-001 Lisbon, Portugal
[4]Instituto de Telecomunicações, DEEC, IST, UTL, Lisbon, Portugal

Abstract

Friction Stir Welding (FSW), as well as others solid state welding processes, frequently originate micro defects of less than 100 micron depth. The morphology and location of these defects lead to a high loss of mechanical properties of the welded joints, particular under fatigue. Moreover, actual NDT reliability in characterizing and sizing these defects still remains a challenge. This paper reports the development of an innovative eddy current (EC) probe, and its application to FSW. The new EC probe presents innovative concept issues, allowing 3D induced current in the material, a lift-off independence, and an easy interpretation of the signal based on a comprehensible qualitative change. The new EC probe was performed on standard defects and aluminium alloys processed by FSW. All results were compared with conventional helicoidally and planar spiral EC probes. The results allow concluding that the new EC probe is able to detect and sizing micro root defects on FSW with 60 micros depth.

Introduction

New demands for NDT techniques are incoming associated with the increase of industrial applications of welding by friction stir (FSW) [1], which is one of the most remarkable development in the recent history of production technologies. In FSW the work pieces are joined by the interaction of a rotating non-consumable tool, which is plunged and traversed along the joint line. It is a solid state welding processes, that proceeds below the melting point of the weld material, *i.e.,* there is no bulk melting in the region of the joint. As a consequence, very good quality welds can be achieved, without common defects of fusion welding processes, namely: porosities and lack of fusion [2].

Although this quality improvement, some imperfections may arise on FS welds, due to improper stirring of the parent material, inadequate surface preparation, lack of penetration of the pin, or inadequate axial forging forces. Some typical FS weld imperfections include i) incomplete penetration, ii) root imperfections (weak or intermittent welding), iii) cavities (typically on the advancing side), and iv) particles alignment (oxides and second phase particles) under the shoulder processed zone, or in the nugget (e.g. sillys), as well as in the weld root. From the scope of these imperfections, the root defects (i and ii) are the ones more difficult to be detected, and that present

higher loss of mechanical resistance of the joints under fatigue loading [3]. Therefore these are the target defects on FSW non-destructive inspection.

In fact, the quality assessment of FSW presents a paradigm in NDT, mainly due to the micro root defects. This type of defects may exhibit a particular morphology (Figure 1), characterized by i) very low size (typical < 100 µm), ii) no physical material discontinuities, iii) very low energy reflection effect, and also iv) electric conductivity changes due to the FSW process itself, even with no defects [4]. This adverse morphology makes the detection of the FSW micro root defects hard difficult or even impossible with actual NDT solutions available in the market.

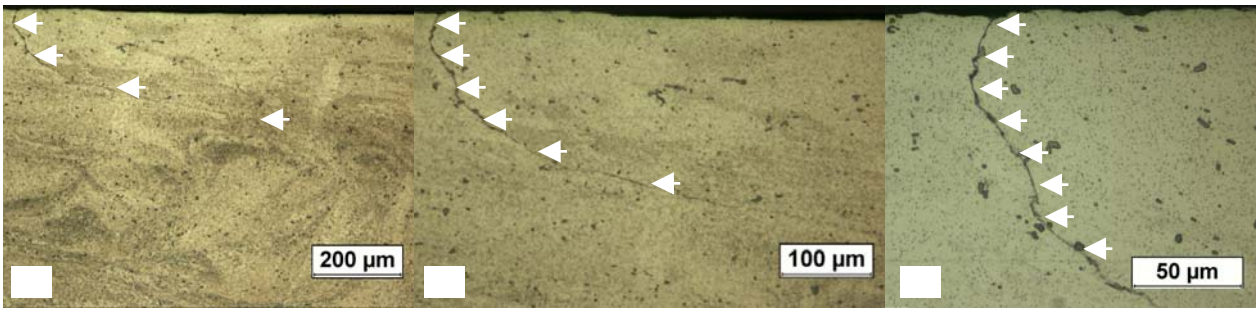

Figure 1 – Transversal FS weld macrography on AA6013-T4 with typical root defects on butt joint.
a) 10x zoom, b) 20x zoom, c) 50x zoom.

Some authors have been made some researches enforce to find reliability NDT techniques to detect and sizing the micro root defects on FSW. Nevertheless, in conductivity materials, when high reliability is required as mentioned before, eddy current is the most adequate technique. However, EC flow can change not only due to defects, but also due to the variations of the probe lift-off. The high-sensitive lift-off effect of conventional EC probes introduces noises which mask the signal of small defects, making their detection difficult or even impossible. Moreover, the low sensitivity of common EC probes as well as other electronic issues may not enable to distinguish between defect and non defective conditions.

Catalin Mandache et al. [5] applied PEC in FSW, but even in the presence of significant size root defects the inspection accuracy is low. PEC variant has the capability to detect deeper defects, nevertheless micro-defects in FSW can hardly be detected. Neil Goldfine et al. [6] have developed a MWM® probe which is able to detect some FSW defects, but only quite large (typically above 150 micron). A. Lamarre et al. [7] was one of the firsts to apply phased array ultrasonic on FSW, and P. H. Johnston et al. [8] has shown the difficulties in detecting the oxides alignment defects on the nugget of the FSW using this NDT technique.

A New Eddy Current Probe

In order to improve the reliability in FSW non-destructive inspection a new NDT EC probe was developed and tested in different FSW defects conditions. The new EC probe allows a 3D induced eddy currents in the material; deeper penetration; independence of the deviation between the probe and the material surface; and easy interpretation of the output signal based on a comprehensible qualitative change.

The so called IOnic probe is constituted by one excitation filament, in the middle of two sensitive planar coils, in a symmetric configuration (Figure 2). Due to this layout the operation of the IOnic probe is based on an integration effect along each sensitive coil, and simultaneous, on a

differential effect between the two coils. The probe was manufactured on 1.6 mm dual layer FR4 PCB subtract with an external diameter of 11 mm. The two sensitive coils are formed by tracks of 100 µm width separated by same dimension gaps.

In Figure 5 it is shown the qualitative eddy current display of the IOnic Probe comparing to an axis-symmetric EC probe. In the IOnic configuration, eddy current flux flows parallel to the excitation filament in the surface plane, but it flows also in other non parallel planes, collinear with the axis of the excitation filament, in a radial arrangement.

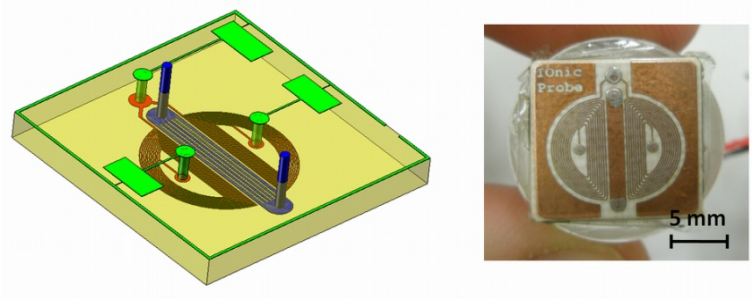

Figure 2 – The IOnic Probe prototype.

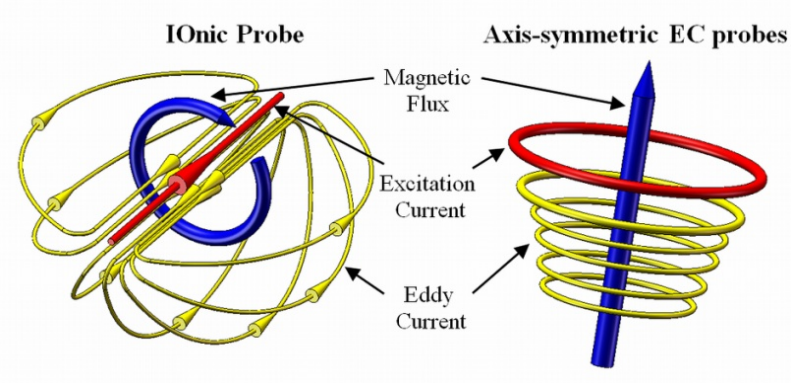

Figure 3 – Eddy currents display in IOnic Probe (left) and conventional axis-symmetric EC probes (right).

The IOnic probe has some other advantages when compared to the conventional eddy currents probes: i) precision differential based operation resulting on high sensibility and superior lift-off immunity; ii) improved contact with test material by being planar, leading to deeper eddy currents penetration in test material; iii) the straight eddy currents induced in the material near the driver trace can be taken as advantage to evaluate materials where the flaws tend to follow a specific orientation; iv) allow the inspection of the material borders as long as the symmetry axis remains perpendicular to it; v) can be implemented in flexible substrates easily adaptable to non-planar and complex geometry surfaces.

Numeric Simulation

A numeric simulation using Finite Element Method (FEM) was created to model the probe and to verify the eddy currents disposition inside the test material. The probe model shown in Figure 3 was developed in CST EM Studio software [9]. The analysis was performed using a hexahedral mesh of 1.22×10^6 elements with local refinement. The probe was placed in the air 300 µm above a

piece of aluminum. A sine wave with 1 A amplitude and frequency of 50 kHz is flowing in the excitation filament. Eddy currents are drawn when the phase of the sine wave is equal to 0º.

When the magnetic stimuli are created around the excitation filament, eddy currents appear in the material as a reaction to oppose this magnetic field. As is shown in Figure 3 b) eddy currents describe loops passing underneath the excitation filament and circular paths defined through the material. Along the symmetry axis, the induced eddy currents take the opposite direction of the current flowing in the driver trace. This eddy current field pattern in the surface of the material, in each side of the excitation filament, is repeated in the interior of the material along the vertical plane. These numerical results validate the eddy currents display illustrated in Figure 3.

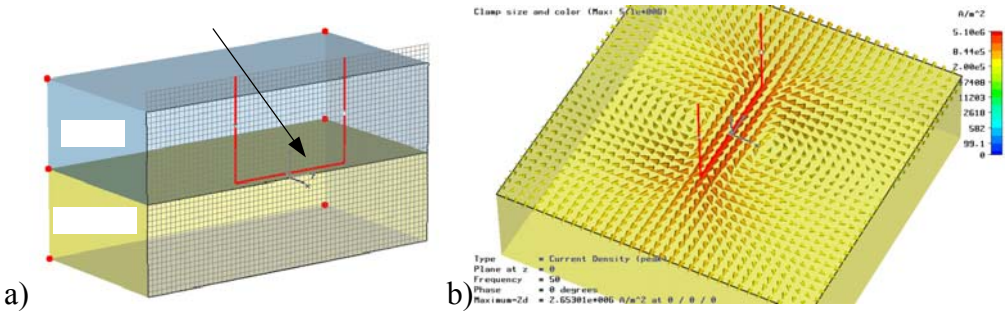

Figure 4 – Numerical simulation of IOnic probe.
a) Geometric model and mesh, b) Vectorial eddy current field on the surface @ f = 50 kHz.

Characterization of FSW defects samples

It was produced three different root defect conditions in AA2024-T351 plates with 3.8 mm thickness: Type 0, Type I and Type II (Table 1 and Figure 5). The three different conditions present a consecutive increase of the defect intensity, suitable for a reliability analysis of a NDT system.

Table 1: Characterization of the tree different FSW produced defects

Defect	Morphology
Type 0	Is characterized by some residual particles alignment in an intermittent path along ≈ 150 µm. This condition is typically considered a non defective weld.
Type I	Subsist a weak or intermittent welding since the materials are in close contact, under severe plastic deformation, but with no chemical or mechanical bond along ≈ 50 µm.
Type II	Defect with ≈ 200 µm non welded zone, followed by particles alignment in an intermittent path.

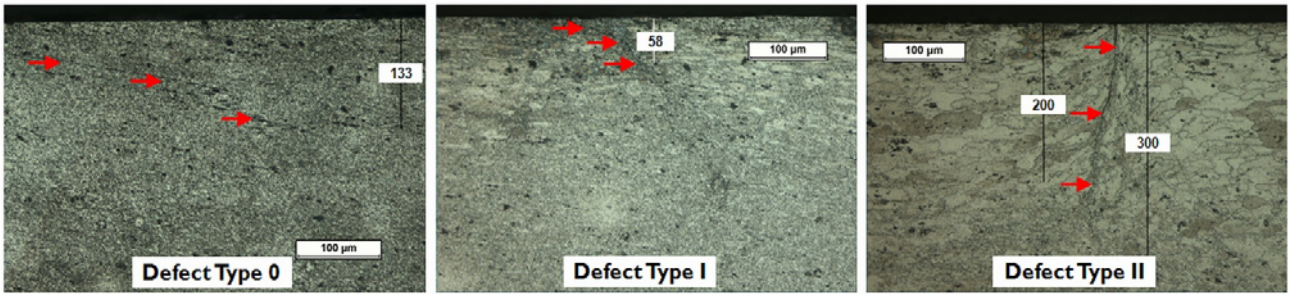

Figure 5 – Transversal macrographs of three different FSW root defects conditions.
Defect Type 0: particles alignment, Defect Type I: ≈ 60 µm, Defect Type II: ≈ 200 µm.

Results

The IOnic Probe was applied on defects condition described before. The data $S(x) = \mathrm{Im}\{\bar{U}_{out}/\bar{I}\}$ was acquired from the root side, along a sweep on the transversal direction to the weld joint, with the excitation filament of the probe parallel to weld joint. The inspection was perform @ $f = 50$ kHz, $f = 100$ kHz and $f = 250$ kHz. The imaginary part of the three types of defects at these frequencies is shown in Figure 6.

As FSW process causes material conductivity changes, even without imperfections, the weld bead is responsible for the large curve on the imaginary part. The presence of imperfections creates a small perturbation observed on the middle of the joint, highlighted in red. This small perturbation observed at the middle of the joint concerns to the suddenly decrease of conductivity due to the local root defect of each defect condition. Notice that there is a very good proportionality between the defect dimension and the observed perturbation on the imaginary part $\mathrm{Im}\{\bar{U}_{out}/\bar{I}\}$. These results show that IOnic probe is able to identify the three different types of defect conditions.

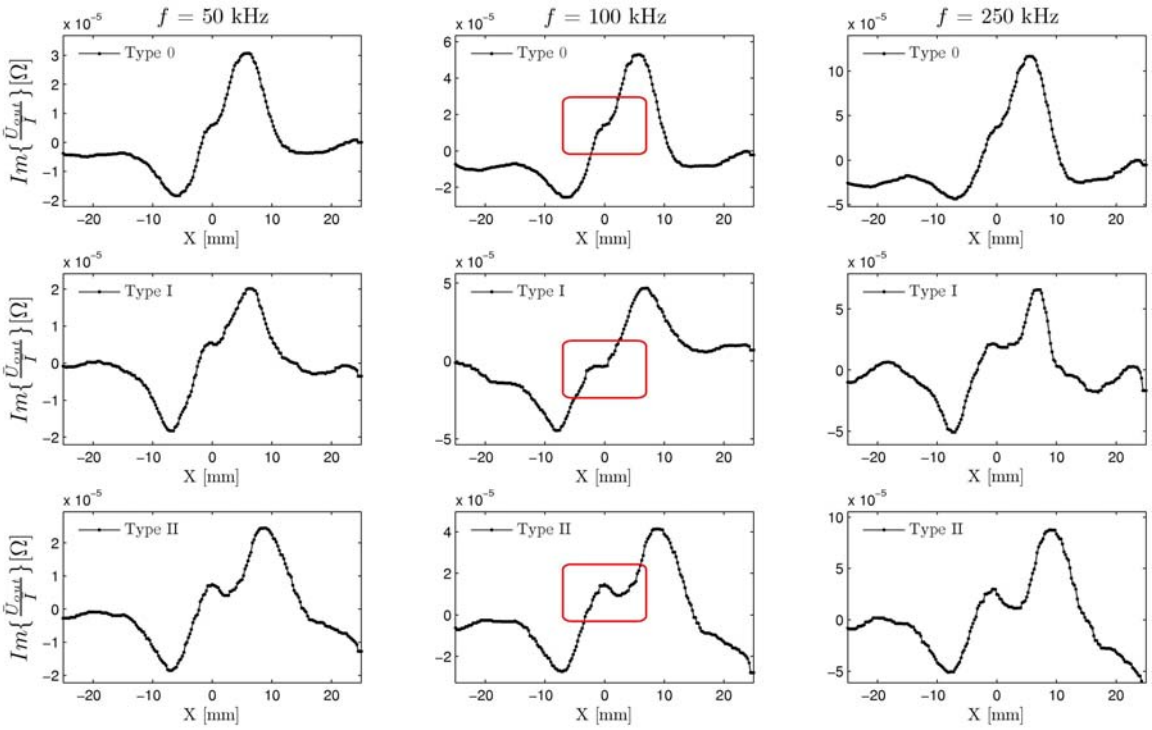

Figure 6 – Results of IOnic Probe for the FSW joints with defect types 0, I and II @ $f = 50$ kHz, $f = 100$ kHz and $f = 250$ kHz.

The same three FSW defect conditions presented in Figure 5 were tested under the same operating conditions using a conventional planar circular spiral EC probe with 20 coils (Figure 7 b). The spiral probe has an outside diameter of 9 mm and coils of 50 µm width separated by the same dimension gaps. In Figure 7 a) it is presented the obtained results $S(x) = \mathrm{Re}\{Z\}$ @ $f = 250$ kHz. The three curves present a very similar trend between them. In fact, unlike the IOnic probe there is no distinctive signal feature that can allow to distinct between each defect condition. Indeed, the absolute planar spiral probe can only reproduce the global spreaded increase of conductivity field due to the FSW bead. Such probes are not able to distinguish small suddenly variations of conductivity, caused by a local root defect with small size. These results compared to the IOnic probe results illustrate the difficulty of NDT of FSW when using conventional EC probes.

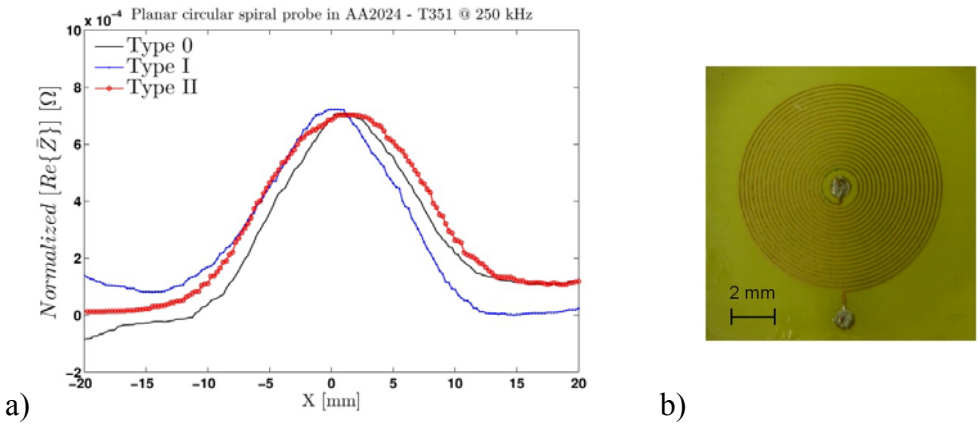

Figure 7 – Results of conventional eddy current probes.
a) Defect types 0, I and II @ f = 250 kHz using a planar circular spiral probe,
b) Conventional planar circular spiral probe with 20 coils and an outside diameter of 9 mm.

Conclusions

In this paper a new EC probe was introduced and tested on FSW of AA2024. The results were compared with a planar spiral EC probe. Conventional axis-symmetry EC probes such as planar circular spiral probes are not able to distinguish FSW micro root defects with depth below 200 μm. The experimental results shown that the IOnic probe is able to identify different levels of FSW root defects, by a qualitative perturbation of the output signal. It was also shown that exist a good proportionality between the defects size and this signal perturbation.

Acknowledgments

The authors would like to acknowledge the Portuguese Fundação para a Ciência e a Tecnologia (FCT) for its financial support via the PhD scholarship FCT – SFRH/BD/ 65860/2009.

References

1. International patent Nº PCT/GB92/02203, Inventors: W. M. Thomas, December, 1991.
2. Telmo Santos, Pedro Vilaça, Luísa Quintino, "Developments in NDT For Detecting Imperfections in Friction Stir Welds in Aluminium Alloys", Welding in the World, Vol. 52, N.º 9/10, pp. 30-37, 2008.
3. T. Santos, P. Vilaça, L. Reis, L. Quintino, M. de Freitas, "Advances in NDT Techniques for Friction Stir Welding Joints of AA2024", in The Minerals, Metals & Materials Society (TMS), Vol. 3, New Orleans, 2008, pp. 27-32.
4. T. Santos, P. M. Ramos, P. Vilaça, "Non destructive testing of friction stir welding: Comparison of planar eddy current probes", *IMEKO TC4 Symp*osium, Florence, Italy, pp. 507-512, September, 2008.
5. C. Mandache, L. Dubourg, A. Merati, *Materials Evaluation*, 4, 382-386 (2008).
6. D. Grundy, V. Zilberstein, N. Goldfine, "MWM-Array Inspection for Quality Control of Friction Stir Welded Extrusions", in *ASM 7th International Conference on Trends in Welding Research*, Pine Mountain GA, 2006, pp. 16-20.
7. A. Lamarre, M. Michael, "Phased array ultrasonic inspection of FS Weldments", in *Review of Progress in Quantitative Nondestructive Evaluation*, AIP Conference Proceedings, Vol. 509, American Institute of Physics, 2000, pp. 1333-1340.
8. P. H. Johnston, "Addressing the Limit of Detectability of Residual Oxide Discontinuities in Friction Stir Butt Welds of Aluminum Using Phased Array Ultrasound", NASA Technical Report, 2008.
9. CST EM STUDIO® (CST EMS), Low Frequency Electromagnetic Design and Simulation, http://www.cst.com/Content/Products/EMS/Overview.aspx.